INSTITUTE OF PHYSICS PUBLISHING JOURNAL OF PHYSICS B: ATOMIC, MOLECULAR AND OPTICAL PHYSICS

J. Phys. B: At. Mol. Opt. Phys. **35** (2002) 691–700 PII: S0953-4075(02)29780-1

Associative ionization in hydrogen atom–rare gas collisions between 10 and 100 eV

B Brehm and P Wilhelms

Institut für Atom- und Molekülphysik, Abteilung Atomare Prozesse, Universität Hannover, Appelstrasse 2, 30167 Hannover, Germany

E-mail: wilhelms@ceres.amp.uni-hannover.de

Received 9 October 2001, in final form 16 November 2001
Published 31 January 2002
Online at stacks.iop.org/JPhysB/35/691

Abstract

We have observed the process of associative ionization (AI) in collisions between hydrogen and rare gas atoms both prepared in their ground states ($H + X \longrightarrow XH^+ + e^-$ with X = Ar, Kr, Xe). This is the first experimental observation of this process, which we compare to the other charge-producing cross sections reported previously. AI takes place only in a small region of collision energies close to threshold. The cross sections show a distinct maximum, with a typical value of about 2×10^{-19} cm^2. In contrast to the heavier rare gases AI is not observed in collisions of atomic hydrogen with He and Ne.

1. Introduction

Charge production processes in collisions of neutral particles have been investigated in our laboratory for many years. Primarily the experimental data are of practical interest in astrophysics, e.g. in stellar atmospheres. On the other hand, the data give information about nonadiabatic mechanisms leading to these processes. There are extensive collections of experimental results on such collisions [1, 2]. Most of these data belong to the energy range above 500 eV, but only rarely are data given at lower energies, especially close to threshold. For ionization processes in collisions between hydrogen atoms and the heavier rare gases (H + X with X = Ar, Kr, Xe) experimental data are available, down to energies as low as 20 eV [3–5]. In this energy range the only charge production processes occurring in hydrogen–rare gas collisions with ground state atoms are ion pair formation

$$H + X \longrightarrow H^- + X^+$$

and free electron production

$$H + X \longrightarrow H^+ + e^- \qquad \text{or} \qquad H + X \longrightarrow X^+ + e^-.$$

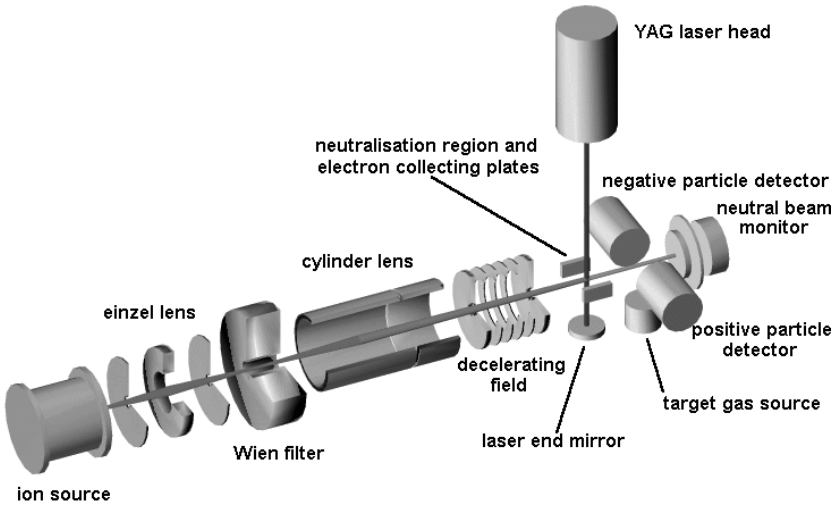

Figure 1. Principle of the neutral H beam production. H atoms are formed by photodetachment of negative ions inside the cavity of a YAG laser. The ion beam, and consequently the neutral beam, are focused by the cylindrical lens into the scattering volume.

Though the associative ionization (AI) $H + X \longrightarrow HX^+ + e^-$ cannot be observed in collisions above 20 eV it is a well known process in collisions with metastable rare gas atoms at thermal energies [6–8].

The first AI process with particles in their ground states has been observed in the system $H + H_2$ at collision energies between 10 and 15 eV [9]:

$$H + H_2 \longrightarrow H_3^+ + e^-.$$

The present paper reports the first observation of AI in collisions of H atoms with rare gas atoms, both in their ground states. Our results include some additional data for other collisional ionization processes below 30 eV. For all cross sections the absolute values (in cm^2) are given.

2. The experiment

The experimental method used has been described previously [9]. In short: the atomic hydrogen beam, adjustable in an energy range from 10 eV to several hundred eV, is crossed by a target beam from a multichannel jet. The scattering volume is located in the electric field of a coincidence time-of-flight difference mass spectrometer. The time difference between the detection of the two charged particles from an ionizing collision gives all the information needed to identify the particles. For the present experiments the range of laboratory energies of the H atom beam was extended down to 10 eV by carefully adjusting and optimizing all components relevant to this beam, most importantly the beam monitor.

The neutral atomic hydrogen beam is generated by laser photodetachment from a H^- beam (see figure 1). These ions are produced in a NH_3 gas discharge, accelerated to 600 eV and focused by an electrostatic einzel lens onto the exit slit of a Wien filter that transmits only H^-. Another lens refocuses the pure H^- beam into the scattering volume and an electric field along the beam axis decelerates the ion beam to the desired energy. Before reaching the scattering volume the H^- beam crosses the cavity of a 1.06 μm YAG laser where up to 20% of the ions are neutralized by photodetachment. The current of detached electrons is used as

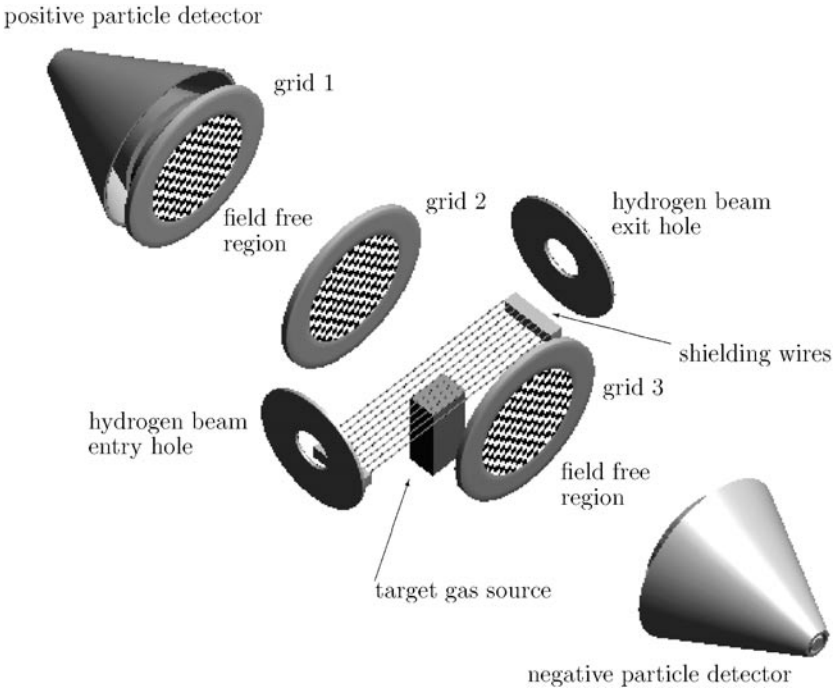

Figure 2. Principle of detection. Charged particles formed in the scattering volume are accelerated in the electric field produced by grids 2 and 3. The field-free regions between these grids and the detectors make certain that the time of flight of the particles is independent of the position of their formation.

a measure of the neutral beam intensity. The remaining ions are deflected by an electric field and thus separated from the neutral beam. A beam monitor, consisting of two multichannel plates (MCP), a luminous screen and a video camera, allows excellent control of the neutral beam profile and position. Working with H beam energies below 20 eV is difficult because with decreasing energy the divergence of the beam increases and the sensitivity of the monitor decreases. Both restrict the reliable beam control rigidly to the region above 10 eV. The energy relevant for the collision process is not the H beam energy E_H but the kinetic energy of the relative motion E_{rel} of the colliding particles: $E_{\mathrm{rel}} = E_H M_T/(M_H+M_T) \pm E_T$, where M_H and M_T are the masses of the H atom and the target and E_T is the contribution of the target motion to the collision energy E_{rel}. The scaling factor $M_T/(M_H + M_T)$ is of minor importance for the results given in this paper, but was quite helpful for the discovery of the AI process in collisions between H atoms and H_2 molecules [9]. E_T is also quite unimportant here, because the target atoms have only thermal kinetic energy at 300 K and because the multichannel jet limits the opening angle of the target beam effectively to $\pm 10^\circ$ about the direction perpendicular to the H beam. Thus E_T adds only a small contribution to the effective width of the collision energy, given by the H beam energy width of less than 0.2 eV. The energy scale may have an additional uncertainty of up to 0.2 eV due to contact potentials.

The H beam is crossed by the target beam (He, Ne, Ar, Kr, Xe) effusing from a multichannel array. Figure 2 shows the scattering region. Charged particles generated in the scattering volume are accelerated in a homogeneous electric field of 2.7 kV cm^{-1} perpendicular to the neutral beam axes. Positive and negative particles are separately registered by two MCP detectors. The time delay between the detection of two particles generated in the same reaction depends on their masses. In our case the measurement of this time delay leads to an explicit

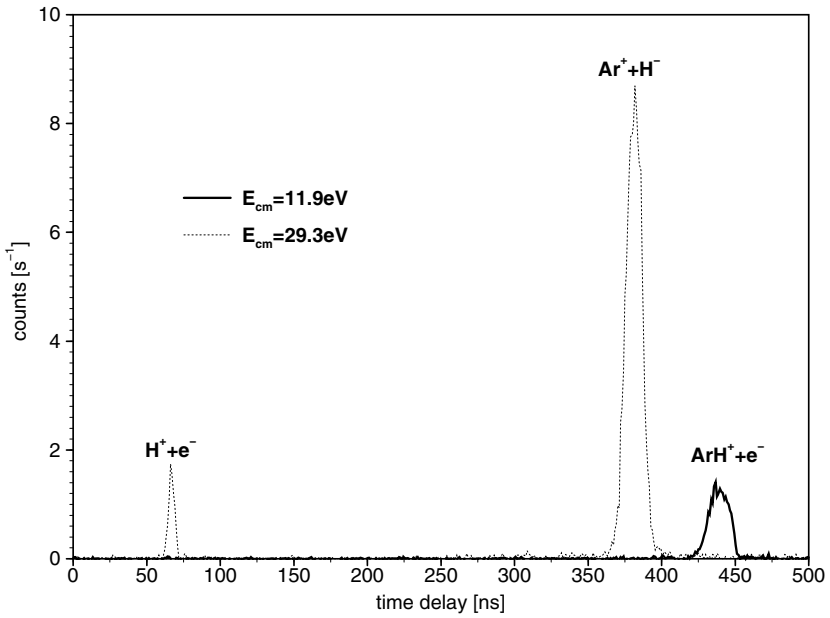

Figure 3. Time-of-flight difference spectra for the system H + Ar. At a collision energy of 29.3 eV (· · · · · ·) two peaks appear, belonging to the product pairs $H^+ + e^-$ and $Ar^+ + H^-$. At 11.9 eV (——) only one peak appears, indicating the product pair $ArH^+ + e^-$ formed by AI.

identification of the detected pairs. In our measurements the essential quantity is the count rate of detected charged pairs as a function of the time delay. Figure 3 shows an example.

The electric field in the collision region (see figure 2) produced by grids 2 and 3 is large enough to lead all charged particles produced onto the detectors independent of their mass, charge, initial direction and initial velocity, as long as the kinetic energy of the colliding particles is below 100 eV. Since the density n_T of the target beam is constant across the H atom beam profile (with beam flux I_H), which is closely controlled, any energy dependence of the measured coincidence count rate $N_{co,i}$ can be attributed to the energy dependence of the corresponding integral cross section σ_i, which is given by the following expression:

$$\sigma_i = \frac{N_{co,i}}{n_T I_H L \eta_{i+} \eta_{i-}}$$

where L denotes the length of the scattering region and η_{i+}, η_{i-} are the detection efficiencies of positive and negative particles, respectively, formed in the process i.

False signals, coming from collisions of the H atoms with the background gas, were separately measured and subtracted. Spurious signals from other sources, such as photons or other particles from the ion source, are also subtracted or have been checked and confirmed to be negligible.

For the target gas density n_T only an order of magnitude estimate can be given in our experimental arrangement. In order to determine the size of the integral cross sections as a function of the collision energy two calibration steps have to be carried out.

(i) The sensitivity of the two particle detectors, which depends on the type of particle detected, has to be measured.

(ii) For every collision pair one of the partial cross sections or the total cross section for charge production has to determined absolutely (in cm^2) for one collision energy at least.

For the first calibration step a method has been used which was developed at our laboratory [10, 11]. By measuring the count rates of both charged particles produced and simultaneously the coincidence count rate, the detection efficiency for both charged products can be obtained as the ratio of the coincidence count rate and the count rate of the other charged collision product. To employ this method great care has to be taken to avoid the detection of any charged particle not produced in the process under investigation or to subtract these false contributions.

For the second calibration procedure absolute cross sections from the literature were used because, with our experimental setup, no trustworthy method to determine the target gas density is known.

All cross sections presented in this paper have been calibrated by these methods.

3. Experimental integral cross sections

3.1. H + He and H + Ne

For these systems our measurements cover the energy range between 10 and 100 eV. Figure 4 shows the integral cross sections as a function of the collision energy. In the energy range below 100 eV in both systems H + He and H + Ne the only observed charge-producing process is H atom ionization

$$H + He(Ne) \longrightarrow H^+ + e^-.$$

The absolute values were obtained by using the experimental results of van Zyl [12] and Fleischmann [13] for calibration (see table 1). For energies below 100 eV the charge production cross sections $\sigma_\pm$ given by these authors are identical to those for H atom ionization.

The cross sections of both systems are very similar to each other in shape and size. In the range between 30 and 70 eV the cross sections increase by two orders of magnitude and the absolute values reach $\approx 1.5 \times 10^{-18}$ cm^2 at 80 eV collisional energy, in agreement with earlier results [4, 12, 13] within experimental error.

Though the energies needed for the two processes (ion pair production $He^+(Ne^+) + H^-$ and target ionization $He^+(Ne^+) + e^- + H$) are both below 25 eV these processes are not observed in our range of collision energies; they have been observed, however, at much higher energies [14].

For these two collision systems our measurements give the first cross sections for ionization processes in collisions of ground state atoms below 50 eV. But, apart from these data our most remarkable result is the absence of AI or any other charge-producing process at energies below 20 eV, i.e. the cross sections are smaller than $\approx 2 \times 10^{-21}$ cm^2. This is an essential difference from the other hydrogen–rare gas systems.

Table 1. Reference data taken from van Zyl *et al* [12] and Fleischmann *et al* [13] used to obtain the absolute values of the cross sections. The data points given are used in a least squares fit to calibrate our cross section curves (see figure 4).

Process	E_{rel} (eV)	σ (10^{-18} cm^2)	Error (%)	Reference
$H + He \longrightarrow H^+ + e^-$	80	1.1	$< \pm 40$	[12, 13]
	70	0.8	$< \pm 40$	[13]
	64	0.8	$< \pm 40$	[12]
	56	0.5	$< \pm 40$	[12]
$H + Ne \longrightarrow H^+ + e^-$	95	1.9	$< \pm 30$	[13]
	67	0.8	$< \pm 25$	[13]
	43	0.3	$< \pm 25$	[13]

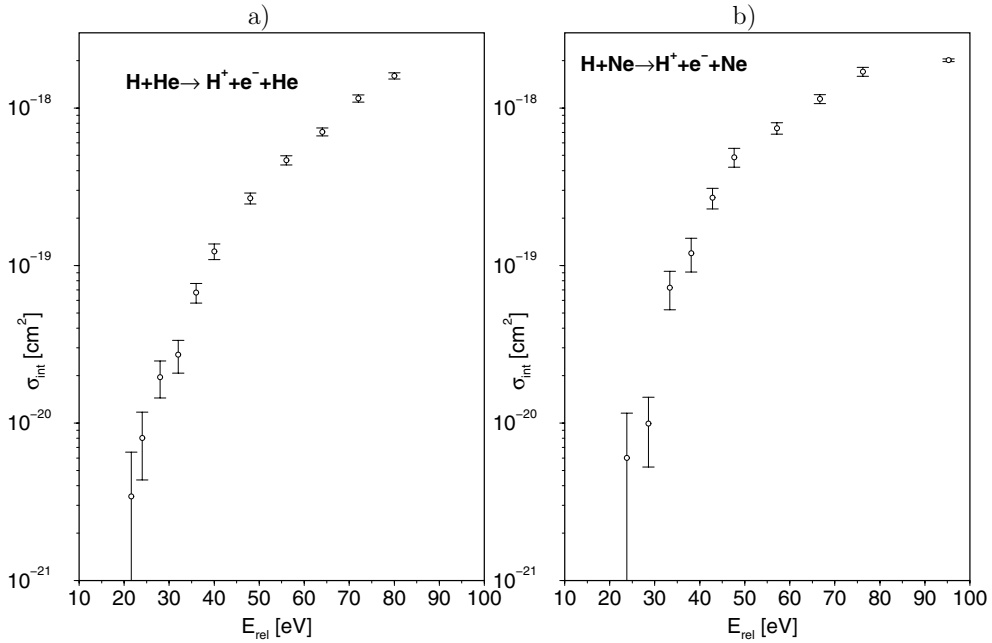

Figure 4. Integral cross sections for ionizing collisions in the systems H + He and H + Ne as a function of collisional energy. Below 100 eV there is only one ionization channel open leading to the product pair $H^+ + e^-$. The error bars indicate the relative uncertainty of our data points (± 1 standard deviation). The absolute scale obtained by adjusting our results to the literature data (see table 1) may have an error up to 50% which is not included in the error bars.

Table 2. Reference data used to obtain the absolute values of the cross sections. We used the values given by Aberle *et al* [3] as reference data, but his calibration is based on the experimental results of van Zyl *et al* [15] and Fleischmann *et al* [16].

System	Ionization channel	E_{rel} (eV)	σ (10^{-18} cm^2)	Error (%)	Reference
H + Ar	$Ar^+ + H^-$	30	1.6	±25	[3]
	$Ar^+ + H^-$	63	4.7	±20	[15]
H + Kr	$Kr^+ + H^-$	25	2.2	±25	[3]
	All	80	11	±25	[16]
H + Xe	$Xe^+ + H^-$	30	5.0	±25	[3]
	All	80	5.9	±25	[16]

3.2. H + Ar, H + Kr and H + Xe

For these systems we present integral cross sections for collisional ionization processes with energies below 30 eV. Our results are shown in figures 5 and 6. The absolute cross section values are also based on the data of van Zyl *et al* [15] and Fleischmann *et al* [16]. However, since the range of collision energies covered by these authors does not overlap with ours, we used the curves published by Aberle *et al* [3] for the production of rare gas ions to bridge the energy gap between the data of van Zyl *et al* or Fleischmann *et al* and our measurements. The reference data are given in table 2. This extrapolation procedure may introduce an additional error. So we estimate that the absolute values for the cross sections are in error by no more than a factor of 2.

Rare gas atom target ionization (Ar^+, Kr^+, $Xe^+ + e^-$) cannot be observed at such low collision energies. Using Ar or Kr as targets both ion pair formation and hydrogen ionization are

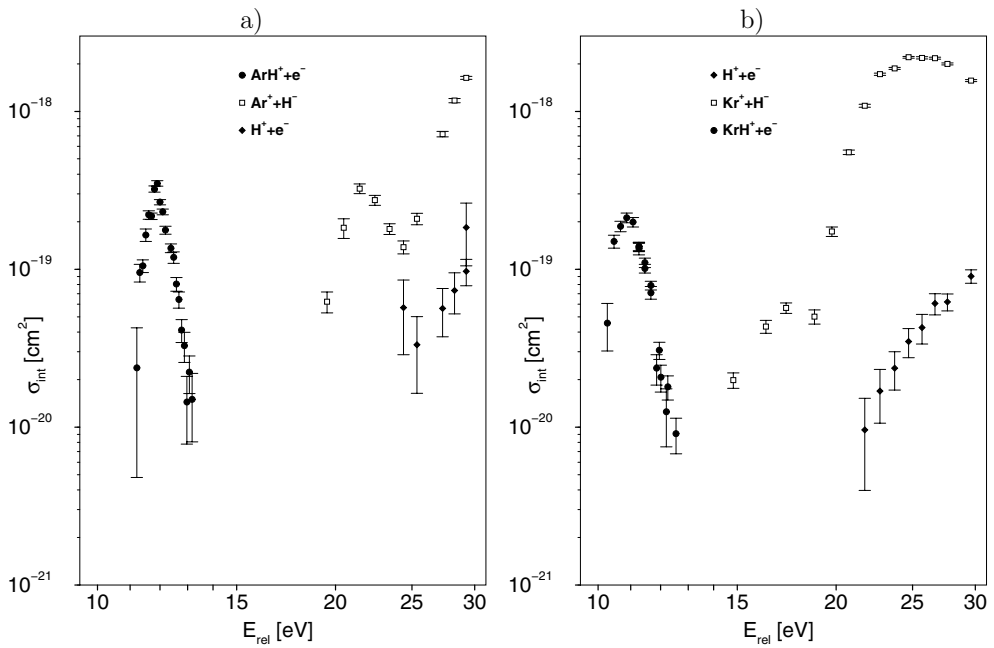

Figure 5. Integral cross sections for ionizing collisions in the systems H + Ar and H + Kr as a function of collisional energy. For the uncertainties see figure 4. Due to the calibration procedure the uncertainty of the absolute scale must be estimated to a factor of 2.

Table 3. Thresholds and energetic region of AI. Theoretical thresholds are obtained by subtracting the proton affinities [17] of the rare gases from the ionization energy of hydrogen.

Process	Threshold (eV)	Observed at (eV)	Maximum value (cm^2)
$H + Ar \longrightarrow ArH^+ + e^-$	9.8	$11.3 < E < 13.2$	3.5×10^{-19}
$H + Kr \longrightarrow KrH^+ + e^-$	9.2	$10.3 < E < 12.6$	2.1×10^{-19}
$H + Xe \longrightarrow XeH^+ + e^-$	8.4	$E < 11.9$	1.7×10^{-19}

observable at collision energies below 30 eV. In the case of Xe + H the hydrogen ionization does not occur in this energy range but it has been observed at collision energies above 500 eV [2].

The oscillations in the cross sections for ion pair production can be observed not only below 30 eV but in a wide range of energies up to the keV region. A detailed analysis of this phenomenon was published by Grosser *et al* [5].

For the observation of the AI processes it was necessary to extend the measurements as far as possible down to low collision energies. Table 3 gives the threshold energies for these processes. Unfortunately our experimental setup does not allow measurements with H atom energies below 10 eV, because of the limitations of the H beam monitor (see section 2). Since the AI process breaks off at energies around 13 eV its cross section is limited to a few eV between threshold and 13 eV.

In the case of H + Ar and H + Kr there actually exists an energy gap where no charged particles are produced. In collisions with Xe there is a small range of energies around 12 eV where both AI and ion pair production can be observed. But for all systems the vanishing of the cross section for AI with increasing energy cannot be explained by a competing ionization process.

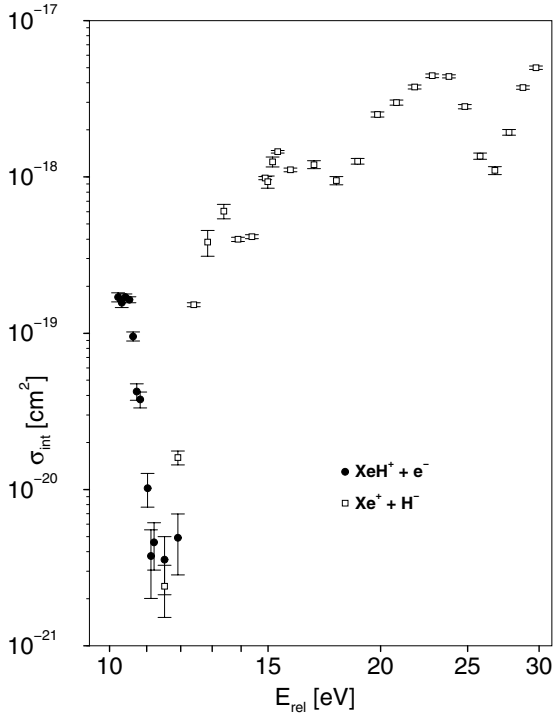

Figure 6. Integral cross sections for ionizing collisions in the system H + Xe. Observed ionization processes are ion pair formation ($E > 11.5$ eV, □) and AI ($E < 11.9$ eV, ●). For the error bars and the uncertainty of the absolute scale see figure 5.

4. Discussion

Integral cross sections for the excitation of H atoms to the $n = 2$ states in H + Ne collisions were calculated by Grosser *et al* [18] and found to agree with the experimental results in a satisfactory way. These authors presented experimental data measured with largely the same apparatus as used in this work. They also presented experimental results on the H atom ionization cross section; in fact, our present work just adds four points to their curve at the low energy end between 20 and 50 eV. So our main result presented here for collisions of H and Ne atoms in their ground states is that the ionization of the H atom is the only process between 10 and 100 eV producing charged particles with an integral cross section of 2×10^{-21} cm^2 or larger. In particular no ionization of the Ne atom is observed, no ion pair production, $Ne^+ + H^-$, and no AI, $NeH^+ + e^-$, in this low energy region. The same is true for H + He collisions. In view of the results of Grosser *et al* [18] we believe that a model including only the molecular states generated with ground state Ne atoms and all states of the H atom should be sufficient to understand all the H atom excitation, including ionization. Such a model may also confirm that all other excitation and ionization processes are negligible below 100 eV. The excited states of the Ne or He atom and the molecular states they generate apparently come into play in collisions with much higher energies only.

This simple picture is not sufficient to explain the experimental results obtained with the heavier rare gas atoms. Experimental data on the cross section of ion pair production, e.g. $Ar^+ + H^-$, were published before [5] and here again the contribution of the present work is only a confirmation and the addition of some extra data points on the cross section curves

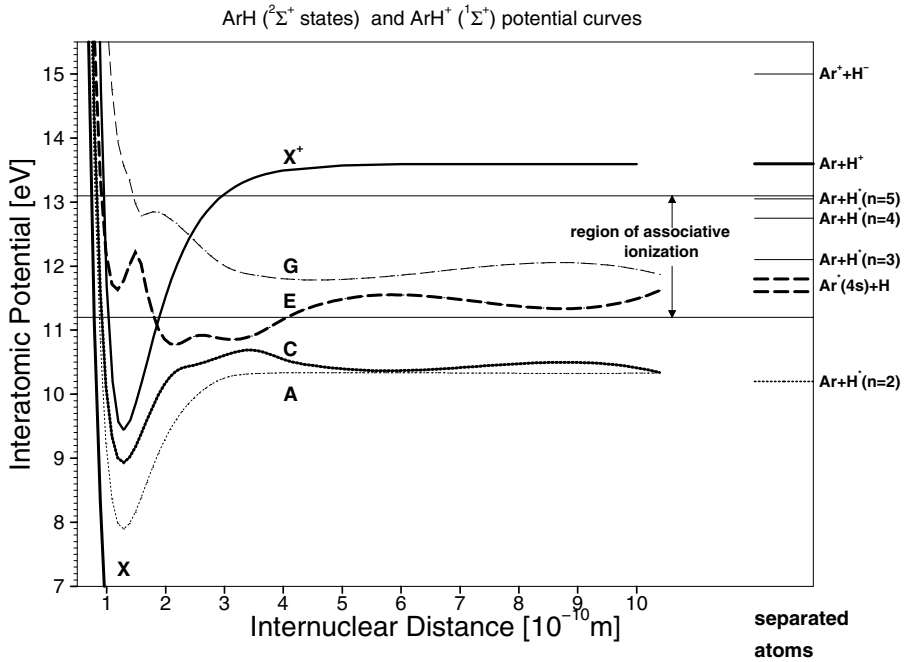

Figure 7. Calculated potential curves for ArH and ArH^+ [20, 21]. Curve ***E*** is correlated with the atomic states $H(1s^1)$ and $Ar(\ldots 4s^1)$ disturbs the Rydberg series, leading to excited H atom states at large internuclear distance.

at low energies. The oscillations observed for all three atoms (Ar, Kr and Xe) can safely be assumed to be Rosenthal oscillations [19]. However, the potential curves generated by excited states of the rare gas atoms are obviously needed here, but they are not well known, especially at higher energies close to the ionization limits. In figure 7 we have collected some calculated potential curves for the ArH system from Vance and Gallup [20] and Toennies [21], which we have preferred because they are available as numerical data. Within the context of a qualitative discussion these curves are adequate and not in contradiction with more accurate calculations of Petsalakis *et al* [22]. Figure 7 shows that the lowest excited Ar state causes a large disturbance among the Rydberg series converging to the ArH^+ ground state and there are many other molecular states connected to excited Ar atoms below the low energy limit of the ion pair production process, so a calculation will not be easy. For Kr and Xe the situation is even more complicated, because for these target atoms the first excited states are even lower than for Ar, in fact below the 2s state of the H atom.

At first sight an explanation for the size and form of the cross section for AI producing $ArH^+ + e^-$ should be easier to find, because it is the ionization process which requires the smallest collision energy. It competes, however, with the process of collisional excitation of the H atom to the $n = 2$ levels, which has a much larger cross section and starts close to its threshold at 10 eV [23]. The AI process, on the other hand, has a lower threshold, of about 9.8 eV, but does not start below 11.3 eV, roughly. So the primary process appears to be a transition from the ground state to the excited molecular state connected to the $n = 2$ states of H. In this lower energy gap between the onset of inelastic collision processes just above 10 eV and the start of the AI process at 11.3 eV the dissociation of the colliding atoms appears to be much faster than the autoionization which could result in stable ArH^+ ions. Starting at 11.3 eV, however, there seems to exist an effective process transferring the molecules into a state from

which they cannot so easily dissociate. This process could be caused by a molecular state connected to excited Ar atoms, like the state labelled $\boldsymbol{E}$ in figure 7. This state could transfer some of the molecules into higher Rydberg states with $n = 4$ or 5 which, produced at collision energies below 12.75 eV, cannot dissociate directly. At 13 eV the AI process breaks off and no charged particles are produced in collisions at energies between 13 and 20 eV. In this higher energy gap again dissociation wins against autoionization, possibly because the dissociation channels leading to H atoms with $n = 4$ and above open up for direct dissociation. Since all the excited states of the He and Ne atoms lie above the ionization limit of H, for these target atoms there is no disturbance of the Rydberg series of molecular states converging to the HeH^+ or NeH^+ ground states, respectively. Transitions into one or the other of these excited molecular Rydberg states therefore lead to excited H atoms by direct dissociation, as has indeed been observed in the case of Ne [18], but not to molecular ions, because the probability for an autoionizing transition from an unperturbed Rydberg state into the ionization continuum, to which it belongs, is too small to compete with the process of direct dissociation.

We think that it would be worthwhile to clear up the mechanisms that lead to the observed form and magnitude of the cross sections for AI, because similar phenomena have been observed in the case of collisions of H atoms with molecules like N_2 and H_2O and in many cases the AI process is the ionization process requiring the smallest collision energy. The theoretical effort, however, will not be small.

Acknowledgments

We would like to thank Hartmut Hotop for bringing the process of AI to our attention, Joachim Grosser for many discussions and for suggesting improvements to the manuscript and the Deutsche Forschungsgemeinschaft for supporting this work on inelastic collisions of H atoms over many years.

References

[1] Tawara H 1978 *At. Data Nucl. Data Tables* **22** 491–525
[2] Nakai Y, Shirai T, Tabata T and Ito R 1987 *At. Data Nucl. Data Tables* **37** 69
[3] Aberle W, Brehm B and Grosser J 1978 *Chem. Phys. Lett.* **55** 71–4
[4] Aberle W, Grosser J and Krüger W 1979 *Chem. Phys.* **41** 245–55
[5] Aberle W, Grosser J and Krüger W 1980 *J. Phys. B: At. Mol. Phys.* **13** 2083–97
[6] Lorenzen J, Hotop H and Ruf M-W 1980 *Z. Phys.* A **297** 19–23
[7] Merz A, Ruf M-W, Hotop H, Movre M and Meyer W 1994 *J. Phys. B: At. Mol. Opt. Phys.* **27** 4973–90
[8] Sarpal B-K 1993 *J. Phys. B: At. Mol. Opt. Phys.* **26** 4145–54
[9] Brehm B, Doering J-E, Grosser J, Harms J, Ruscheinski T and Zimmer M 1995 *J. Phys. B: At. Mol. Opt. Phys.* **28** 1517–25
[10] Brehm B, Grosser J, Ruscheinski T and Zimmer M 1995 *Meas. Sci. Technol.* **6** 953
[11] Oberheide J, Wilhelms P and Zimmer M 1997 *Meas. Sci. Technol.* **8** 351–4
[12] van Zyl B, Le T-Q and Amme R-C 1981 *J. Chem. Phys.* **74** 314–23
[13] Fleischmann H-H and Young R-A 1969 *Phys. Rev.* **178** 254–60
[14] Roussel F, Pradel P and Spiess G 1977 *Phys. Rev.* A **16** 1854–60
[15] van Zyl B, Le T-Q, Neumann H and Amme R-C 1977 *Phys. Rev.* A **15** 1871–86
[16] Dehmel R-C, Meger R and Fleischmann H-H 1973 *J. Chem. Phys.* **58** 5111–16
[17] Hunter E-P-L 1998 *J. Phys. Chem. Ref. Data* **27** 413
[18] Grosser J, Schnecke A and Voigt H 1990 *Z. Phys.* D **17** 251–5
[19] Rosenthal H and Foley H-M 1969 *Phys. Rev. Lett.* **23** 1480–3
[20] Vance R-L and Gallup G-A 1980 *J. Chem. Phys.* **73** 894–901
[21] Gianturco F-A, Niedner G, Noll M, Semprini E, Stefani F and Toennies J-P 1987 *Z. Phys.* D **7** 281–8
[22] Petsalakis I-D and Theodorakopoulos 1994 *J. Phys. B: At. Mol. Opt. Phys.* **27** 4483–9
[23] Grosser J, Krüger W, Steen W and Voigt H 1990 *J. Phys. B: At. Mol. Opt. Phys.* **23** 959–79